NUMERICAL ANALYSIS OF A VORTEX CONTROLLED DIFFUSER

Robert E. Spall
Department of Mechanical Engineering
University of South Alabama
Mobile, AL 36688

SUMMARY

A numerical study of a prototypical vortex controlled diffuser is performed. The basic diffuser geometry consists of a step expansion in a pipe of area ratio 2.25:1. The incompressible Reynolds averaged Navier-Stokes equations, employing the $K - \varepsilon$ turbulence model, are solved. Results are presented for bleed rates ranging from 1 to 7 percent. Diffuser efficiencies in excess of 80 percent are obtained. Reattachment lengths are reduced by a factor of up to 3. These results are in qualitative agreement with previous experimental work. However, differences in some basic details of experimentally observed and the present numerically generated flowfields exist. The effect of swirl is also investigated.

INTRODUCTION

The central idea behind the vortex controlled diffuser (VCD) is that highly efficient diffusion may be achieved by bleeding off fluid through a small gap located at a region of rapid expansion. This concept appears to have been first introduced by Heskestad [1]. In that work, edge suction was applied through a slot situated at the edge of a convex corner. It was found that the flow turned the corner in a manner that significantly decreased the extent of the recirculation region. Heskestad later [2] experimented with edge suction at the step expansion of a circular pipe, evaluating the effectiveness of the configuration as a short diffuser. That study employed a uniform inlet profile with a thin boundary layer. Heskestad also [3] considered the effectiveness of edge suction in producing a short diffuser when the inlet profiles were fully developed. High static pressure recoveries were produced in both cases.

The desirability of a short diffuser between the compressor and combustor in gas turbine applications provided the incentive for further development of the VCD concept. Adkins [4] obtained data for a series of research diffusers with area ratios ranging from 1.9:1 to 3.2:1. He found that, for moderate bleed rates, efficiencies in excess of 80% could be achieved with diffuser lengths 1/3 that required with conventional conical diffusers. A hybrid diffuser (a combination VCD and conventional diffuser) was later studied by Adkins et al. [5]. Results showed that bleed rates were reduced from those required for the previously studied step VCD configurations. Most recently, Sullerey et al. [6] have investigated the effect of inlet flow distortion on a VCD. Results revealed that as inlet distortions were increased, so too were the levels of bleed required to maintain diffuser efficiency.

It appears that the only previous numerical work concerning the VCD was performed by Busnaina and Lilley [7]. In that work, the incompressible Navier-Stokes equations were solved

for the flow in a two-dimensional VCD geometry. Although the effects of turbulence were not modeled, and the grid employed was quite coarse, the general trends followed those observed experimentally.

The mechanism by which the VCD operates is still unclear. One explanation is that a region of high shear is produced resulting in a layer of turbulence that inhibits flow separation [4]. Others [3] have suggested that the primary result of suction is to simply deflect or turn the mean flow around the sharp corner, thus diminishing the length of the recirculation zone.

In the present work the performance of a prototypical VCD is investigated numerically. The incompressible, axisymmetric Reynolds averaged Navier-Stokes equations are solved for the flow through a pipe containing a step expansion of area ratio 2.25:1. The vortex chamber and bleed gap height-to-length ratio are representative of those employed in previous experimental works. The effect of turbulence is modeled using the $K - \varepsilon$ model. (The standard $K-\varepsilon$ model has predicted the reattachment length for flow in a sudden pipe expansion within experimental uncertainty [8]). Calculations are performed for bleed rates ranging from 1% to 7%. For comparative purposes, results for a step expansion without the benefits of bleed are also presented. Details of the flow structure are studied and presented using velocity vectors and contour plots of pressure, turbulence kinetic energy, and axial velocity.

NUMERICAL APPROACH

The incompressible Reynolds-averaged Navier-Stokes equations are appropriate to describe the motion within a prototypical VCD configuration. Although the governing equations are solved in cylindrical polar coordinate form, for purposes of brevity they are presented below in cartesian tensor form. The continuity and momentum equations are given as:

$$\frac{\partial u_i}{\partial x_i} = 0 \tag{1}$$

$$\frac{\partial u_i}{\partial t} + u_j \frac{\partial u_i}{\partial x_j} = -\frac{1}{\rho}\frac{\partial p}{\partial x_i} + \frac{\mu}{\rho}\nabla^2 u_i - \frac{\partial R_{ij}}{\partial x_j} \tag{2}$$

respectively, where u_i is the mean velocity, ρ is the density, μ is the viscosity, p is the mean pressure and $R_{ij} = \overline{u'_j u'_i}$ are the Reynolds stresses. The Boussinesq hypothesis provides an expression for the Reynolds stresses in terms of the gradients of the mean flow [9] as:

$$-R_{ij} = -\frac{2}{3}\delta_{ij}K + \frac{\mu_t}{\rho}(\frac{\partial u_i}{\partial x_j} + \frac{\partial u_j}{\partial x_i}) \tag{3}$$

where μ_t is the turbulent viscosity and K is the turbulent kinetic energy. The turbulent viscosity is expressed, in terms of K and the dissipation rate, ε, as:

$$\mu_t = \rho C_\mu \frac{K^2}{\varepsilon} \tag{4}$$

382

Transport equations for K and ε, respectively, are given as [10]:

$$\frac{DK}{Dt} = \frac{\partial}{\partial x_i}\left(\frac{\nu_t}{\sigma_k}\frac{\partial K}{\partial x_i}\right) + \nu_t\frac{\partial u_i}{\partial x_j}\left(\frac{\partial u_i}{\partial x_j} + \frac{\partial u_j}{\partial x_i}\right) - \varepsilon \tag{5}$$

$$\frac{D\varepsilon}{Dt} = \frac{\partial}{\partial x_j}\left(\frac{\nu_t}{\sigma_\varepsilon}\frac{\partial \varepsilon}{\partial x_j}\right) + C_1\nu_t\frac{\varepsilon}{K}\frac{\partial u_i}{\partial x_j}\left(\frac{\partial u_i}{\partial x_j} + \frac{\partial u_j}{\partial x_i}\right) - C_2\frac{\varepsilon^2}{K} \tag{6}$$

It remains to specify the empirical constants in the above equations. Although investigators have attempted to optimize these values for recirculating and/or swirling flows (c.f. [8]), most of these attempts have been *ad hoc*, and thus the standard values for boundary-layer flows ($C_\mu = 0.09$, $C_1 = 1.44$, $C_2 = 1.92$, $\sigma_\kappa = 1.0$ and $\sigma_\varepsilon = 1.3$) have been taken. Near the wall, it is assumed that the log-law holds.

The above equations were solved using the commercial code FLUENT [11]. FLUENT uses a control volume technique with non-staggered grids. All variables are stored at control volume centers. QUICK [12] interpolation is used to provide values of the variables on cell faces. Pressure-velocity coupling is implemented using the SIMPLE [13] algorithm. Convergence of the solution is assumed when the normalized residual for each conservation equation is decreased to 10^{-3}. (The residual for a given equation consists of the summation of the unbalance in the equation for each cell in the domain.) Since the above solution techniques are well known and widely discussed in the literature, they will not be elaborated upon here.

GEOMETRY AND BOUNDARY CONDITIONS

A prototypical axisymmetric VCD of expansion area ratio 2.25:1 is considered (see Figure 1). (The radius of the diffuser upstream of the expansion is 1 unit; downstream, 1.5 units.) The diffuser geometry is typical of that employed in dump combustors. The essence of the diffuser is the suction slot at the expansion corner. Small quantities of fluid (typically 5% of the mass flow) are bled off through the suction slot into a vortex chamber. Fluid exits the chamber through a channel (as shown in Figure 1). In the present study, the axial extent of the slot (L) is taken as 0.1 units, and the radial depth (D), 0.05 units. Thus, the slot length-to-depth ratio is 2.0, typical of those employed in experimental works appearing in the literature. The total length of the VCD configuration is 25 units, with the gap beginning 2.4 units downstream from the inflow plane. A length of 25 was chosen so that outflow boundary conditions could be specified with reasonable accuracy. The radius of the pipe upstream of the expansion is 1 unit; the radius downstream, 1.5 units. A cylindrical grid consisting of 85 cells in the axial direction and 45 cells in the radial direction is employed. Cells were clustered toward the vortex fence (the aft wall of the vortex chamber) and the lateral diffuser walls. To assure a grid converged solution, calculations are also performed using double the number of grid points in each coordinate direction (for the 5% swirl case).

For all cases, a uniform inflow axial velocity profile was specified. Previous experimental studies [2, 3] reveal that thin inlet boundary layers result in higher pressure recoveries than fully developed turbulent profiles, and thus it is expected that pressure recoveries in the present study would be somewhat decreased if fully developed turbulent inlet profiles were used. However, the underlying physical principals should not be affected. The Reynolds number, based on inflow pipe diameter and velocity is 200,000. This is representative of Reynolds numbers employed in

most experimental investigations, which range from 100,000 [4] to 840,000 [5]. The inlet turbulence intensity is 10%. Given the turbulence intensity, the turbulence kinetic energy and dissipation rates are calculated from:

$$K = \frac{3}{2}(u')^2 \tag{7}$$

$$\varepsilon = C_\mu^{\frac{3}{4}}\frac{K^{\frac{3}{2}}}{l} \tag{8}$$

where l is a turbulence length scale given as 0.07R, (R is the inlet pipe radius). At the outlet, fully developed flow conditions are assumed; that is, streamwise gradients of the flow properties are set to zero.

RESULTS

Results have been obtained for the VCD with bleed rates ranging from 1% to 7%, and for a step expansion (without the vortex chamber). In addition, results for the 5% bleed case with swirl have been obtained. For the sake of brevity, contour and velocity vector plots are provided only for the case of the step expansion, and the VCD 5% bleed case. In addition, only the portion of the domain near the suction slot is shown. (Note that grey contour lines signify negative values.)

Before delving into a description of the flowfield, it is first desirable to provide some means of quantifying improvements in diffuser effectiveness as a function of bleed rate. Toward this end, a one dimensional correction may be applied to the usual definition of diffuser effectiveness, which results in the expression [4]:

$$\eta = \frac{p_2 - p_1}{\frac{1}{2}\rho\bar{v}_1^2(\alpha_1 - (\frac{1-B}{AR})^2)} \tag{9}$$

where B is the bleed rate, AR is the area ratio and α is a kinetic energy coefficient. For the case of uniform inflow profiles, α equals unity. (For fully developed turbulent flows in circular pipes, $\alpha = 1.05$.) The dramatic effect of bleed on effectiveness is demonstrated in Figure 2, in which effectiveness is plotted as a function of distance downstream from the step expansion (or fence). In the case of the step expansion, the maximum effectiveness reaches approximately 52%, and is not achieved until nearly 20 step heights (H) downstream from the expansion. Maximum effectiveness increases to 67%, 82%, 90% and 92%, for VCD bleed rates of 1%, 3%, 5%, and 7%, respectively. In addition, the distance required for maximum diffusion to take place decreases from approximately 13 H for 1% bleed to 3 H for 7% bleed. The increase in effectiveness begins to asymptote as the bleed rate is increased beyond 5%. For the 3, 5, and 7% bleed rates, losses to friction cause the effectiveness of the diffuser to diminish slowly beyond about 10 H (downstream of the fence). These results are in qualitative agreement with experimental results for both tubular and annular VCD's presented by Adkins [4]. The results do differ in one important aspect. Adkins [4] suggests that at low bleed rates, diffuser effectiveness increases slowly with increased bleed. Then, at some bleed rate, fluid begins to enter the suction slot from the freestream (as opposed to entering over the vortex fence). At this point, diffuser effectiveness increases rapidly with respect

to slight increases in bleed rate. Finally, at some critical rate (described as the rate necessary for the formation of a stagnation point at the top of the fence) increases in effectiveness with increases in bleed rate become minimal. The numerical results however, show no such trends at low bleed rates. That is, at low bleed rates, numerical results indicate that diffuser effectiveness increases gradually with respect to increases in bleed rate.

One benefit of numerical solutions is that detailed flow patterns are obtained. In the remainder of this section, results in terms of contour plots and velocity vectors are examined. Velocity vectors for the step expansion and for the VCD with 5% bleed are shown in Figures 3a,b, respectively. For clarity, the vectors are plotted at every other gridpoint in both the radial and streamwise coordinate directions. The effect of bleed in reducing the extent of the recirculation region is clearly revealed in Figure 3b. A stable vortical structure within the vortex chamber is also clearly indicated. However, most important is the rapid directional change and acceleration of the fluid around the corner under the influence of bleed. For the step expansion, a clean separation from the corner is obtained.

More accurate indications of the extent of the recirculation regions, described by contours of constant axial velocity, are shown in Figures 4a,b. Figure 4a reveals that for the step expansion, the length of the recirculation zone is approximately 7 H. This value is less than the values of 8-9 H reported experimentally [c.f. 14] over a range of expansion ratios. Numerical results using the $K - \varepsilon$ model range from 7-9 H for an area expansion ratio of 4:1 [c.f. 8] which agree fairly well with the experimental results. However, as the expansion ratio diminishes, one might expect the $K - \varepsilon$ model to begin to underpredict the separation length, in accordance with well known results for the 2D backward facing step. Implementation of 5% bleed reduces the length of the separated region to 2.5 H. In addition, the rapid diffusion downstream of the expansion is well illustrated. The diffusion process appears to be nearly complete at a distance of 5 H downstream from the expansion. This correlates well with the optimum length for the diffuser predicted using wall pressure data as shown in Figure 2 (where the efficiency reaches approximately 85%). One also notes an acceleration of the fluid in the near wall region just upstream of the expansion due to the presence of the low pressure vortex chamber. This is followed by a region in which a rapid decrease in the axial velocity of the fluid occurs as it passes over the gap and, due to the expansion, encounters a strong adverse pressure gradient. The net result is the creation of a region of high localized shear.

Contours of constant pressure are shown in Figures 5a,b for the step expansion and VCD geometries, respectively. The pressure variations presented are with respect to a reference pressure located adjacent to the duct inlet (given as p_1 in Equation 9). Figure 5b reveals that, away from the wall, a significant adverse pressure gradient forms upstream of the suction slot. This occurs due to the flux of fluid through the bleed slot. That is, due to mass removal at the slot, the axial flux decreases away from the wall. Nearer the wall, the influence of the vortex chamber results in a decrease in the pressure with a corresponding increase in the axial velocity. A local minimum in the pressure occurs at the slot entrance and thus serves to deflect the oncoming fluid toward the outer wall. Of further interest is the pressure distribution on the back face of the step. Here, the pressure is not constant along the wall (as is the case with the step expansion, Figure 5a) but increases in the radial direction. To assess the effects of grid refinement, shown in Figure 5c are pressure contours computed using a 170 x 90 grid. Only very minor differences in the contours (appearing near the downstream portion of the shown flowfield) are visible. Thus, the original 85 x 45 grid is deemed sufficient for the purposes of this study.

Contours of turbulence kinetic energy are shown in Figures 6a,b. As previously men-

tioned, the region near the slot is one of high shear, and is thus responsible for the generation of considerable turbulence energy, as revealed in Figure 6b. In addition to this local maximum, an additional maximum appears downstream, near the aft portion of the recirculation region. However, the turbulence levels at this downstream point are below the levels near the slot. This may be contrasted to the case of the step expansion, shown in Figure 6a. Here, only one local maximum appears near the aft portion of the recirculation region. In addition, maximum turbulence levels are below those shown in Figure 6b.

Since many practical VCD applications involve some level of swirl in the approach flow, the effect of swirl on VCD flow patterns is briefly investigated. Again, the bleed rate is taken as 5%, and other flow field conditions remain identical to those described earlier. A solid body rotation is superimposed on the axial velocity at inflow such that the ratio of the maximum swirl velocity to axial velocity equals 0.5. This represents a significant level of swirl, although well below that at which reversed flow is expected to occur. Shown in Figure 7a are contours of constant axial velocity. By comparison with Figure 4b, it is apparent that the length of the recirculation region has been diminished. This is consistent with experimental results reported by, for instance, Dellenback [14] for the step expansion with swirl. (Apparently, no experimental or numerical results on VCD performance under the influence of swirl exist in the open literature.) Pressure contours are shown in Figure 7b. One notes that near the axial location of the bleed slot, radial variations in pressure are similar to those for the zero swirl case. However, downstream from this position, a significant radial gradient exists, as one would expect in the case of swirling flows.

DISCUSSION

The numerical results shed light on several points which have been previously discussed in the literature. The existence of a region of high shear (with corresponding turbulence) has been mentioned as one of the physical mechanisms responsible for the drastic improvements in effectiveness of the VCD over the step expansion as a diffuser [4]. That a region of high turbulence is formed near the suction slot is borne out in the present study. However, that this region is necessary or responsible for preventing flow separation seems unlikely. Indeed, the flow separates at the top of the chamber fence. It appears that the primary contribution of the suction slot is to deflect the fluid toward the outer wall.

It has been suggested [4] that at low bleed rates fluid is drawn into the vortex chamber from this lee side of the fence, resulting in only minimal improvement in diffuser effectiveness. For higher bleed rates, it has then been proposed that this process is diminished, eventually resulting in the formation of a stagnation point on the top of the fence. This bleed rate is termed the critical rate. However, results from the present study do not confirm this process. Even at the 1% bleed level, the results indicate that fluid does not enter the chamber from the lee side of the fence. In addition, a sudden increase in efficiency with respect to bleed rate is not observed, regardless of the chosen length of the diffuser.

There are several possible reasons for the discrepancy regarding the details of the process as observed experimentally, and computed numerically. Of primary concern is the ability of the $K - \varepsilon$ turbulence model to accurately predict fine flow details of this complex recirculating flowfield. Perhaps inclusion of a full Reynolds stress model could be of benefit in this respect. The present study does indicate however, that numerical solutions of the Reynolds averaged Navier-

Stokes equations provide a useful tool to aid in the analysis and design of practical VCD configurations.

ACKNOWLEDGEMENTS

REFERENCES

1. Heskestad, G. "An Edge Suction Effect," AIAA J., Vol. 3, 1965, pp. 1958-1961.

2. Heskestad, G., "A Suction Scheme Applied to Flow Through a Sudden Enlargement," J. Basic Eng., Vol. 90, 1968, pp. 541-544.

3. Heskestad, G., "Further Experiments with Suction at a Sudden Enlargement in a Pipe," J. Basic Eng., Sept. 1970, pp. 437-449.

4. Adkins, R.C., "A Short Diffuser With Low Pressure Loss," J. Fluids Eng., Sept. 1975, pp. 297-302.

5. Adkins, R.C., Martharu, D.S. and Yost, J.O., "The Hybrid Diffuser," J. Eng. Power, Vol. 103, 1981, pp. 229-236.

6. Sullerey, R.K., Ashok, V., and Shantharam, K.V., "Effect of Inlet Flow Distortion on Performance of Vortex Controlled Diffusers," J. Fluids Eng., Vol. 114, 1992, pp. 191-197.

7. Busnaina, A.A. and Lilley, D.G., "A Simple Finite Difference Procedure for the Vortex Controlled Diffuser," AIAA-82-0109, AIAA 20th Aerospace Sciences Meeting, Jan. 11-14, Orlando, FL, 1982.

8. Nallasamy, M., "Turbulence Models and Their Applications to the Prediction of Internal Flows: A Review," Computers & Fluids, Vol. 15, 1987, pp. 151-194.

9. Hinze, J.O., Turbulence, New York, NY: McGraw-Hill Publishing Co., 1975.

10. Jones, W.P., and Launder, B.E., "The Prediction of Laminarization with a Two-Equation Model of Turbulence," Internat. J. Heat Mass Transfer, Vol. 15, 1972, pp. 301-314.

11. FLUENT Users Guide, Fluent, Inc., Lebanon, NH

12. Leonard, B.P., "A Stable and Accurate Convective Modeling Procedure Based on Quadratic Upstream Interpolation," Methods in Appl. Mech. Eng., Vol. 19, 1979, pp. 59-98.

13. Patankar, S.V., Numerical Heat Transfer and Fluid Flow, Washington, D.C., Hemisphere Publishing Corp., 1980.

14. Dellenback, P.A., "Heat Transfer and Velocity Measurements in Turbulent Swirling Flows Through an Axisymmetric Expansion, Arizona State University, PhD dissertation, 1986.
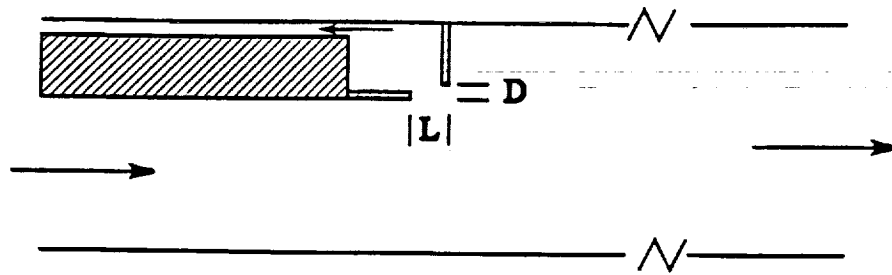
Figure 1   Vortex controlled diffuser geometry.
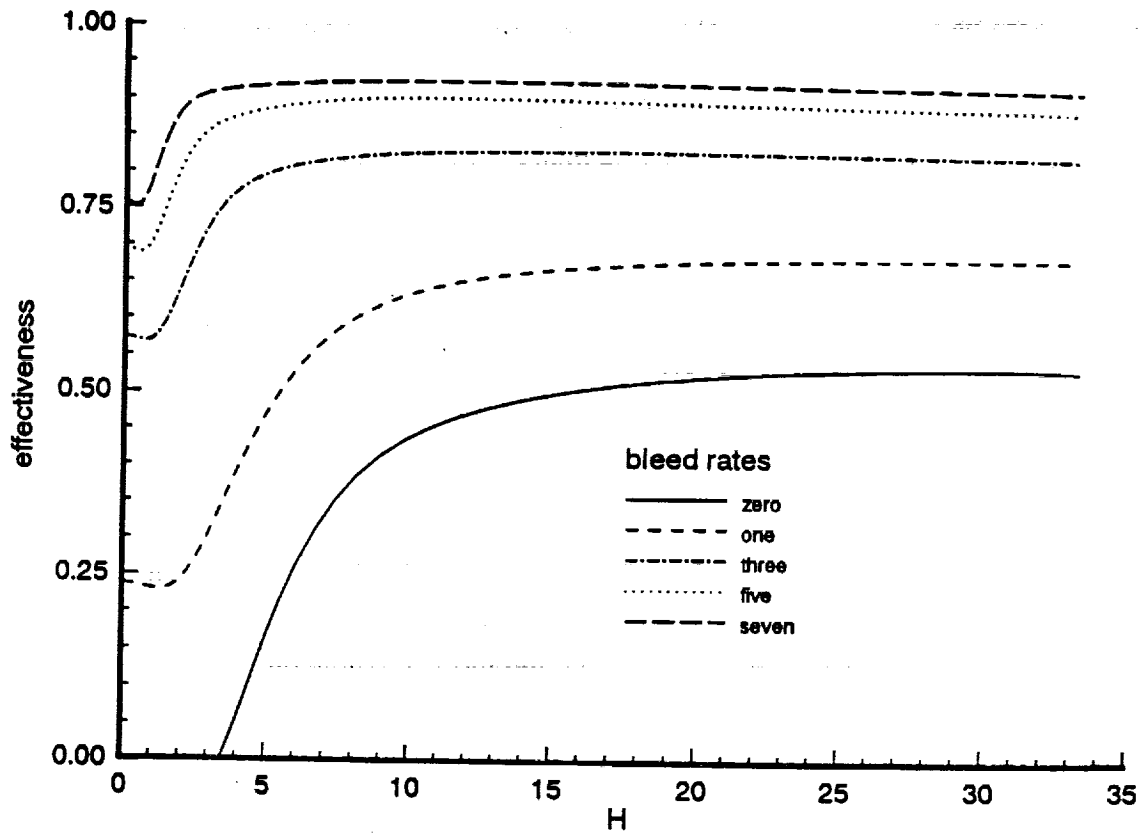
Figure 2   Diffuser effectiveness as a function of the downstream distance from the vortex fence.
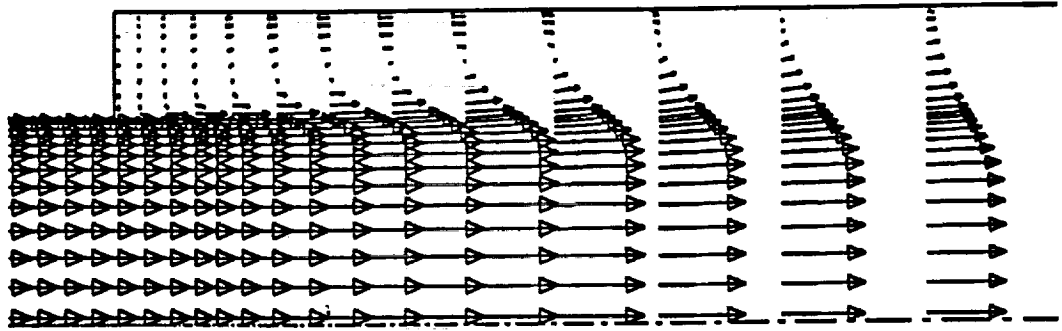
a) step expansion
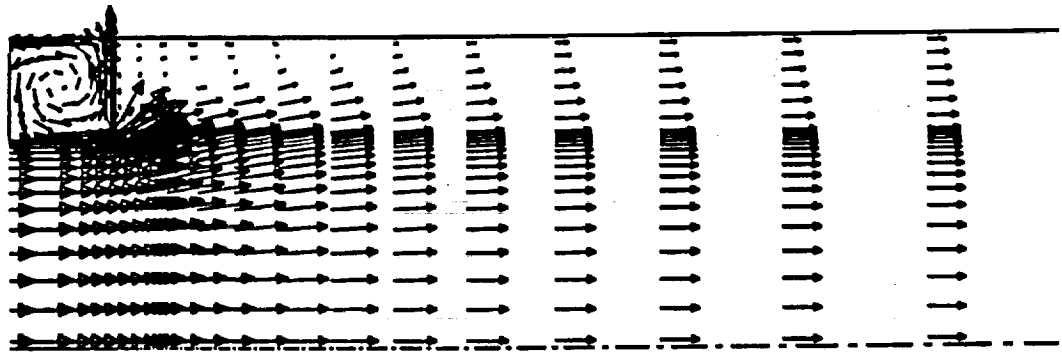
b) VCD with 5% bleed

Figure 3   Velocity vectors in region of step expansion and vortex chamber.
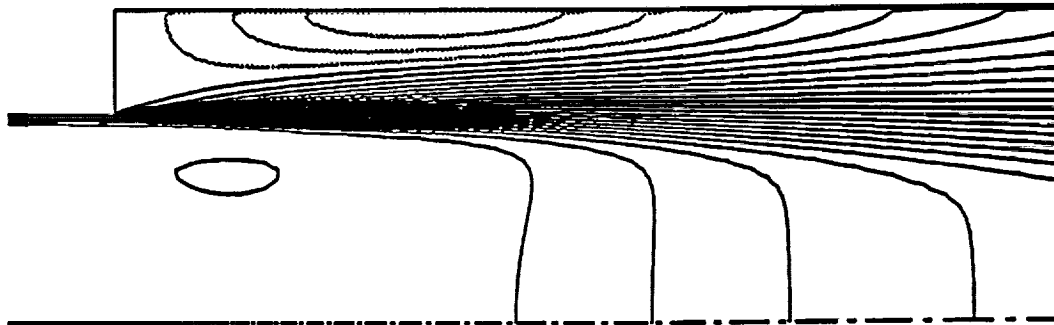
a) step expansion
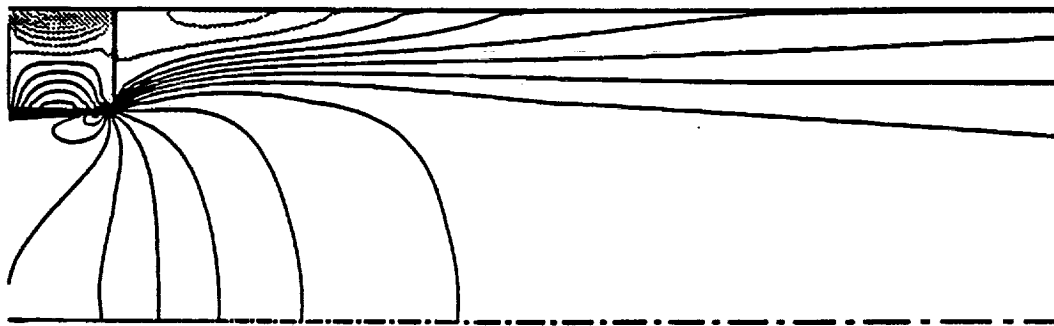
b) VCD with 5% bleed

Figure 4   Contours of constant axial velocity.
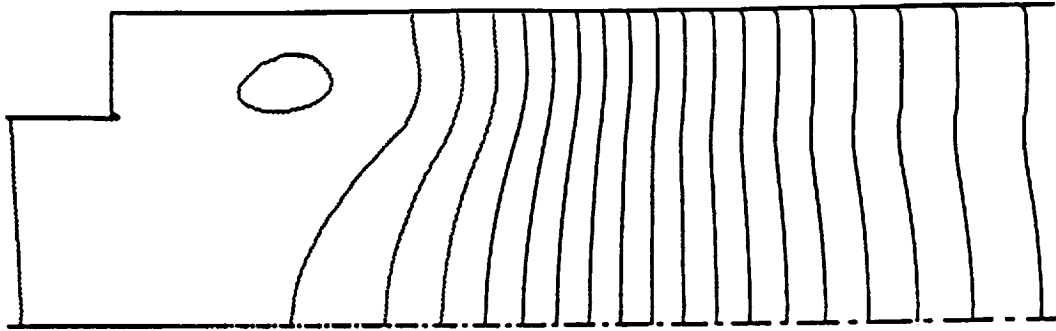
a) step expansion
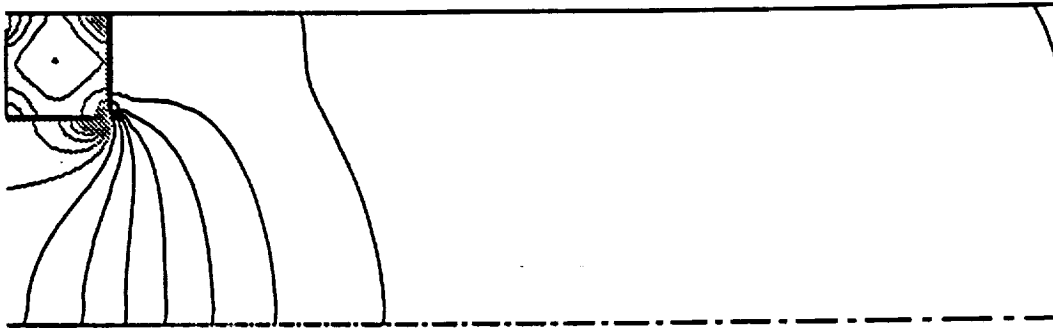
b) VCD with 5% bleed
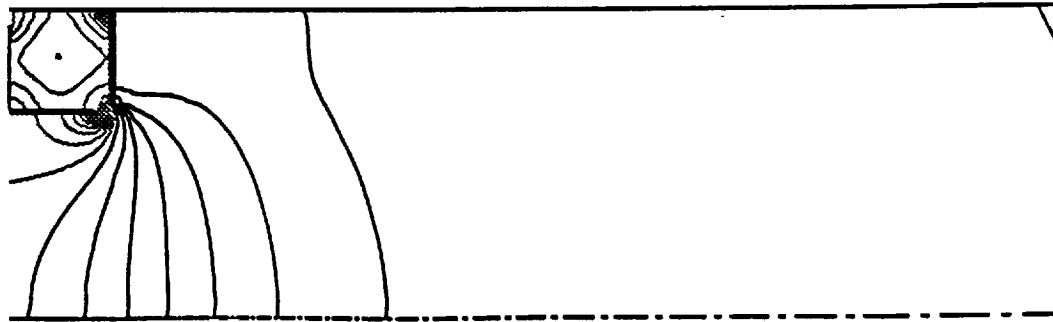
c) VCD with 5% bleed, 170 x 90 grid

Figure 5   Contours of constant pressure.
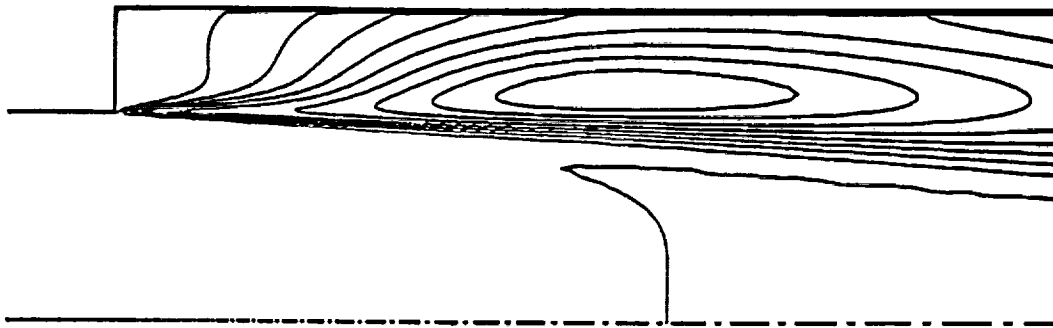
a) step expansion
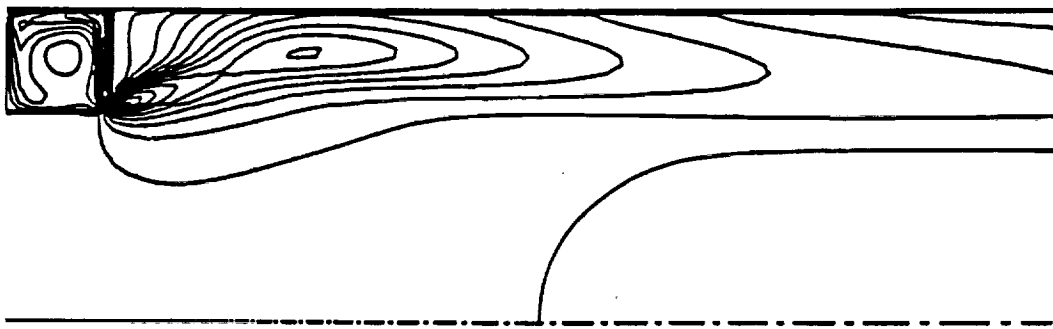
b) VCD with 5% bleed

Figure 6 Contours of turbulence kinetic energy.
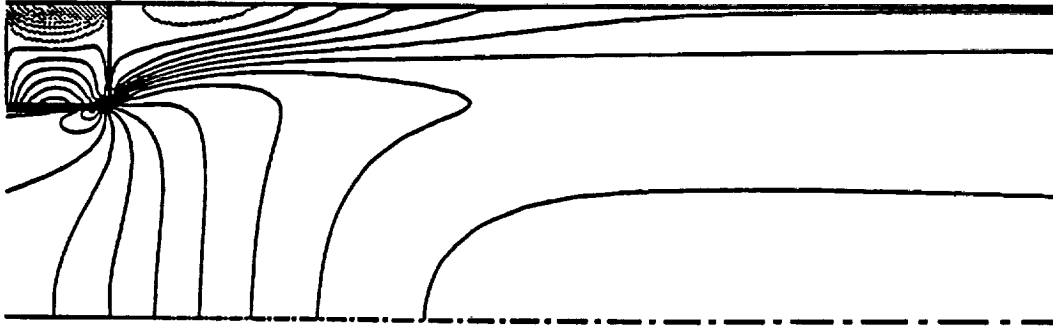
a) contours of constant axial velocity
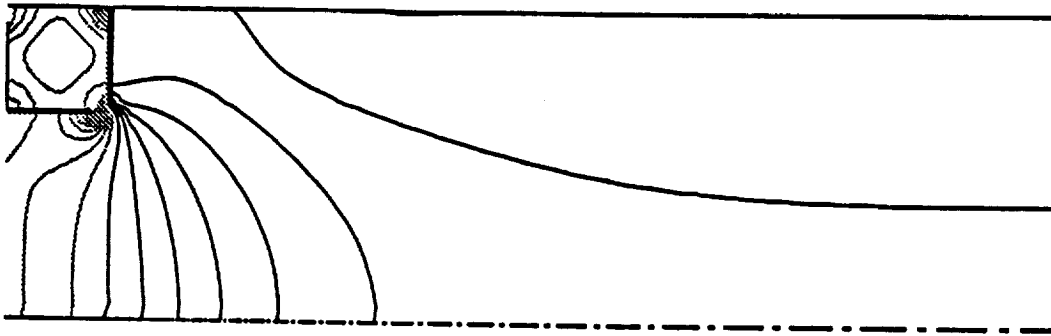
b) contours of constant pressure

Figure 7   VCD with swirl (5% bleed).